PAPER • **OPEN ACCESS**

Modification of the design of circular thin-walled tubes to enhance dynamic energy absorption characteristics: Experimental and finite element analysis

To cite this article: M Ahmad *et al* 2020 *IOP Conf. Ser.: Mater. Sci. Eng.* **917** 012027

IOP Conf. Series: Materials Science and Engineering **917** (2020) 012027 doi:10.1088/1757-899X/917/1/012027

Modification of the design of circular thin-walled tubes to enhance dynamic energy absorption characteristics: Experimental and finite element analysis

M Ahmad[1], K A Ismail[2], M H M Hanid[1], F Mat[3] and A M Roslan[1]

[1]Department of Mechanical Engineering Technology, Faculty of Engineering Technology, Universiti Malaysia Perlis (UniMAP), UniCITI Alam Campus, 02100, Padang Besar, Perlis, Malaysia.
[2]School of Manufacturing Engineering, Universiti Malaysia Perlis (UniMAP), Pauh Putra Campus, 02600, Arau, Perlis, Malaysia.
[3]School of Mechatronic Engineering, Universiti Malaysia Perlis (UniMAP), Pauh Putra Campus, 02600, Arau, Perlis, Malaysia.

masniezam@unimap.edu.my

Abstract. A thin-walled tube is an energy absorber device that functions to dissipate kinetic energy into another form of energy during impact. The design of thin-walled tubes is a significant factor which affects to the energy absorption characteristics. This paper provides a comparative study between the original thin-walled tube designs and several modified tube designs that have been proposed. The main objective is to improve the energy absorption characteristics, such as energy absorption capacity, initial peak load, specific energy absorption (SEA) and crush force efficiency (CFE). Throughout this research, aluminium alloy AA6061-T6 has been used as the material for all tubes. For comparison, all of the tubes are developed with a circular shape with the same diameter, thickness and length. In addition, they are also impacted at the same kinetic energy under dynamic axial loading. Validated LS-DYNA finite element (FE) models have been used to simulate the impact of the thin-walled tubes. Compared to the original tube design, the modified tubes have improved energy absorption characteristics. A conical tube with a flat end cap was identified as the best performing tube among the modified tubes because it had the lowest initial peak load, a moderate energy absorption capacity and an excellent CFE and SEA. The findings from this study can be used as a guidance in designing thin-walled structure.

1. Introduction

Crashworthiness can be defined as the ability of a structure to prevent occupant injuries during an impact [1]. Manufacturers of automobiles, aircraft, ships, railway coaches, lifts and other machinery with moving parts aim to make an improved crashworthy structure to increase occupant safety during an accident. An energy absorber, most commonly a thin-walled tube, is the main component to increase efficiency of a crashworthiness structure. During an accident, the thin-walled tube receives the kinetic energy from the collision and converts it into strain energy through structural deformation, thus minimising the impact experienced by the occupant. In general, the efficiency of the energy absorption is optimum when the thin-walled tube can provide the following characteristics: maximum

energy absorption, specific energy absorption (SEA) and mean crushing force with a minimum initial peak load.

The revolution in the study of thin-walled tube structures was pioneered by Alexander [2], in 1960, with his first analytical model for axial crushing behaviour. With the rapid development of finite element software since last decade, most researchers have adopted this method due to its advantages over conventional methods [3-5]. To compare the effect of different shapes on thin-walled tube energy absorption capacity, Marzbanrad [6], found that the energy absorption capacity for elliptic thin-walled tubes is the greatest, followed by circular and square thin-walled tubes, when impacted under dynamic axial loading. Furthermore, Guler et al. [7] found that conical thin-walled tubes can provide the largest CFE and SEA compared to the square and hexagonal tapered tubes. In addition, Han et al. [8] concluded that 10% of the peak load of a circular tube can be reduced by introducing a cut out into the tube. In addition, Ghamarian et al. [9] attached a metallic plate as the end-cap at the top of a circular tube and found that the cap reduces the initial peak load from 20% until 30% compared to the tube without the end-cap. Previous researchers also noted concerns while studying the effects of foam-filled tubes. Aktay et al. [10] found that extruded polystyrene foam encourages the conversion of the crushing mode of thin-walled tubes from the diamond mode to the concertina mode, with increasing the number of folds and decreasing the fold length during quasi-static loading. Furthermore, Singace [11] concluded that filling the tube with wood, sawdust or chips can enhance the energy absorption capacity and improve the deformation mode from buckling to progressive collapse.

In this paper, a comparative study between the original tube designs and modified tube designs are presented. The original tubes included thin-walled tubes that were manufactured in straight and conical tube shapes. The modified tubes introduced in this paper are also based on the original circular tube geometry. The modifications focus on the making a horizontal cut on the tube, a combination of multiple shapes in a single tube and the addition of a filler inside the tube. The resulting energy absorption characteristics of the original and modified tubes are compared in this study.

2. Finite Element (FE) Modelling

2.1. Development of FE model

Simulations of FE models are conducted using the LS-DYNA explicit software. Figure 1 illustrates the FE model generated in LS-DYNA.

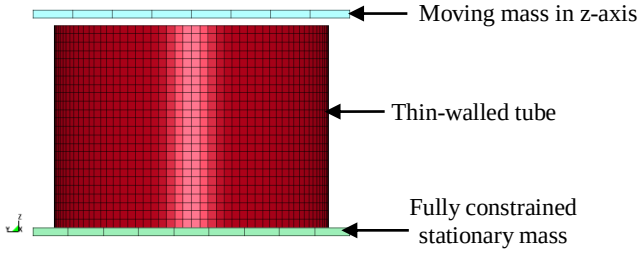

Figure 1. Development of the FE model for the dynamic axial crushing of a thin-walled tube.

In Figure 1, a moving mass is only allowed to translate in the z-axis, while movement along the x- and y-axes are constrained. In addition, rotation of this rigid body is constrained in all directions. Meanwhile, a stationary mass is fully constrained in translation and rotation to support the thin-walled tube during compression. In the early stage, an initial velocity is applied to the moving mass along the z-axis. Then, the moving mass compresses the tube that is supported by the stationary mass with a given velocity. The moving and stationary masses, as illustrated in Figure 1, are modelled using eight node solid elements with a constant stress solid element formulation and a 10 mm mesh size. Material model 020, which refers to a rigid material model, is employed to develop these parts. This material model provides a convenient way to turn these solid element parts into a rigid body [12].

The interface between the moving mass and the tube is generated using "auto nodes to surface" contact. The moving mass is assigned as a master part while the tube is assigned as a slave part with static and dynamic coefficients of frictions of 0.2 and 0.1, respectively, to avoid lateral movements. The same contact type is also applied for the interface between the tube and stationary mass with static and dynamic coefficients of frictions of 0.3 and 0.2, respectively, to avoid lateral movements. "Automatic single surface" contact was activated to avoid penetration between elements throughout the model.

The material of the thin-walled tube is aluminium alloy AA6061-T6 with the following mechanical properties: Young's modulus E = 68.9 GPa, initial yield stress σ_y = 276 MPa, Poisson's ratio v = 0.33, and mass density ρ = 2.7 g/cm3 [13]. The tube is developed by using Belytschko-Tsay shell element formulation with five integration points throughout the thickness. The mesh of the tube is developed by using four-node quadrilateral shell elements, which are suitable for large strain analyses. A 2.0 to 2.1 mm size of the shell element was employed to the tube, based on the previous mesh convergence study conducted by Ahmad et al. [13]. The aluminium alloy tube was modelled using material model 024 (piecewise linear plasticity) in LS-DYNA. This material model is based on the mathematical formulations of the work hardening and strain rate sensitivity. The strain rate effect refers to the Cowper Symonds constitutive equation, which relates the dynamic and static yield stress by the following Equation 1:

$$\sigma_y = \left[1 + \left(\frac{\dot{\varepsilon}}{C}\right)^{\frac{1}{p}}\right]\sigma_0 \tag{1}$$

where σ_y is the initial yield stress, $\dot{\varepsilon}$ is the strain rate, and C and p are the Cowper-Symonds strain rate parameters. The value of C and p for aluminium alloy AA6061-T6 are taken as 6400 ms-1 and 4, respectively, based on the previous study where aluminium alloy AA6061-T6 was found to be strain rate sensitive under dynamic loading [14]. In addition, Table 1 presents the data for the effective plastic strain and the corresponding stress for the quasi-static loading of the aluminium alloy.

Table 1. Effective plastic strain and corresponding stress for aluminium alloy AA6061-T6 [14].

Effective plastic strain (mm/mm)	Corresponding stress (MPa)
0.000	276
0.010	280
0.015	286
0.020	292
0.030	304
0.040	317
0.060	335
0.080	350

The values of these data are used in the Cowper-Symonds equation to introduce the strain rate effect in the dynamic loading simulation. On the other hand, extruded polystyrene foam is used as a filler to be fit into the original straight tube. The extruded polystyrene was prepared in a cubic shape with 50 mm dimensions, and it was compressed with 5 mm/min of crosshead speed according to ASTM D1621-10 [15] by using Universal Testing Machine. In simulation, material model 063 in LS-

DYNA, the crushable foam, was employed in the development of a filler with the mass density, ρ = 0.0361 g/cm3 and Young's modulus E = 0.0149 GPa. The Poisson's ratio is assumed to be zero because there was very little lateral movement measured in the compression test. The engineering stress-strain diagram of the extruded polystyrene (shown in Figure 2) has been applied into the material model 063 in LS-DYNA. The foam elements are created by using the constant stress solid element formulation with a 4.0 mm mesh size. A type 4 hourglass with a coefficient of 0.03 is implemented into the foam. Automatic surface to surface contact is used between the foam and the tube. The automatic node to surface contact is applied between the foam and the moving mass and between the foam and the stationary mass with static and dynamic coefficients of 0.3 and 0.2, respectively.

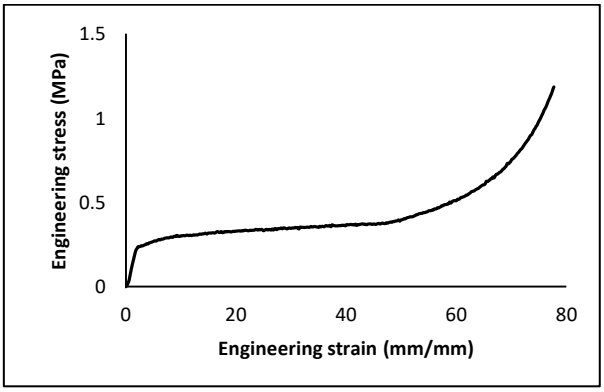

Figure 2. Stress-strain diagram for the extruded polystyrene foam obtained from the quasi-static compression test.

In addition, soft constraint formulation has been employed in the contact algorithm because the soft material (foam) interfaces with the stiff material and the mesh densities between the foam and contacting parts are dissimilar.

2.2. Validation of the FE model

2.2.1. Experimental: Drop impact test. Dynamic loading experiments were performed on the thin-walled tubes in a real environment using a drop weight tower. The experiments were performed under axial loading conditions, as shown in the equipment setup in Figure 3. A thin-walled tube (specimen) was placed at the centre of the support base. The impactor had a mass of 20 kg and was able to move in the vertical direction along the frictionless guide rail. The movement was controlled and supported by a high strength cable from the impactor to the motor. The initial velocity, v, was determined by adjusting the height of the impactor from the top of the specimen by applying conservation of potential and kinetic energy. The specimen was compressed upon contact with the impactor. The acceleration of the impactor was recorded by a Piezotronics accelerometer with a sensitivity of 2.52 g/mV.

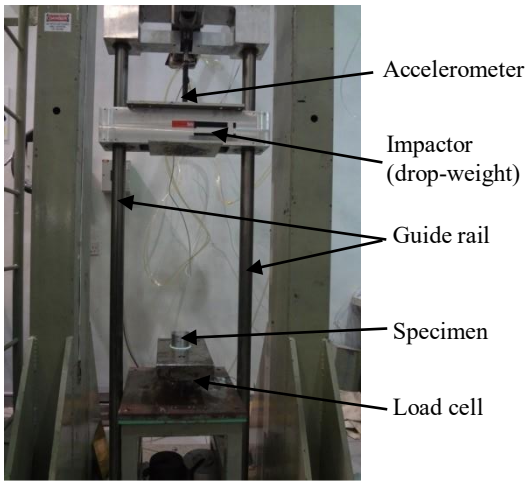

Figure 3. Specimen setup for drop weight test.

In addition, the load applied to the specimen was recorded by the load cell positioned under the support base with a sensitivity of 0.0114 mV/N. The recorded values for these data were filtered and presented using a Yokogawa DL750 oscilloscope with a Kistler charge amplifier. Then, the double integration technique was applied to the recorded acceleration results to plot the force-deformation data to be used for further analysis.

2.2.2. Comparison of the FE model and the experimental results. To ensure the reliability of the FE models, they were compared to the experimental results. Actual geometry, boundary and initial conditions from the experiment, as shown in Table 2, were adopted in the FE model for validation.

Table 2. Specimen dimensions and initial conditions in dynamic loading experiment.

	Specimen 1	**Specimen 2**
Empty/ foam filled	Empty	Foam-filled
Shape	Straight	Conical
Thickness (mm)	0.58	0.50
Bottom diameter (mm)	69.84	69.45
Top diameter (mm)	69.84	60.94
Length (mm)	50.73	50.73
Initial velocity (m/s)	3.38	4.15

Figure 4 (a) and (b) shows the comparison of the force–deformation curves between the experimental and FE model results for the empty straight tube and foam-filled conical tube, respectively. Although there are some differences between the FE model and experimental results, the differences are within the acceptable range of scientific error in a dynamic event with less than 15% of percentage error in overall energy absorption characteristics.

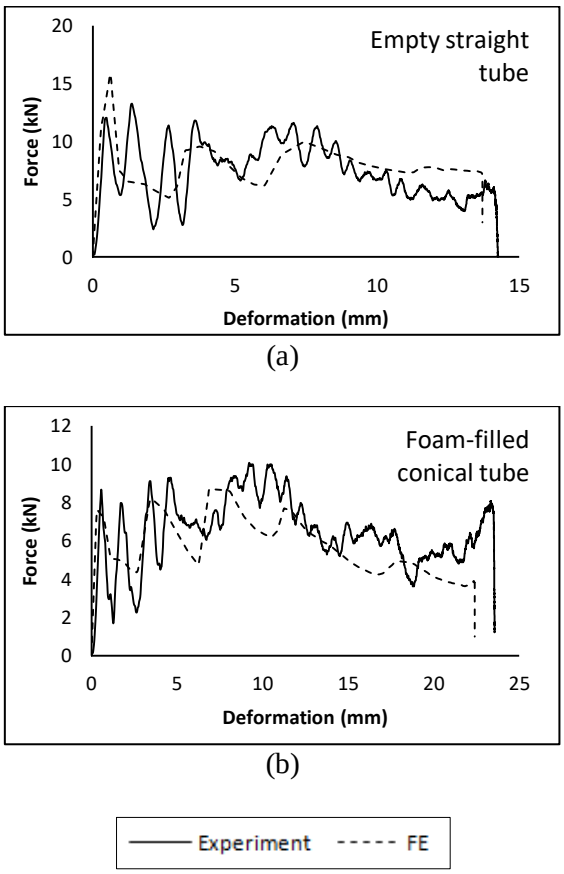

Figure 4. Comparison of force-deformation curves between the experiment and FE model: (a) Empty straight tube, (b) Foam-filled conical tube.

3. Design modifications of thin-walled tubes

Modifications of the original straight and conical tubes are introduced, and the energy absorption characteristics between the original tubes and several proposed modified tubes are compared. To conduct a comparative study between the original tubes and the modified tubes, several parameters were kept constant. Based on the validated model developed in the previous section, all tubes (original and modified) were created using Belytschko-Tsay shell element formulation with a 2.1 mm mesh size. In addition, the total length, diameter and thickness were fixed at 150 mm, 50 mm and 0.5 mm respectively. Furthermore, a combination of 20 kg mass and 10 m/s initial velocity was applied to the rigid body of the moving mass to achieve 1000 J kinetic energy. The energy absorption characteristics for all of the tubes were measured until 110 mm tube deformation length was achieved. Figure 5 illustrates the original and modified tubes and their assigned unique identifications (M1 to M10).

Modification of straight tube	M1 Straight tube (original) 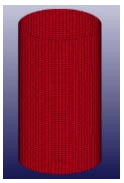	M2 Straight tube with an inclined horizontal cut 	M3 Straight tube with a flat end cap 	M4 Straight tube with a hemispherical cap 
Modification of conical tube	M5 Conical tube (original) 	M6 Conical tube with a flat end cap 	M7 Conical tube with a hemispherical cap 	
Combination of straight and conical tube	M8 Straight tube with conical end 	M9 Straight tube and conical tube with a hemispherical cap 		
Addition of filler into straight tube	M10 Filled straight tube 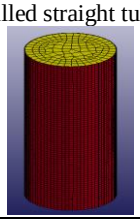			

Figure 5. Design modifications of thin walled tubes.

4. Results and discussion

4.1. Comparisons between a straight tube and a conical tube

An original conical tube (M5) was designed with a 5° semi-apical angle. The thickness, bottom diameter and length were similar to that of the straight tube (M1). Thus, the comparison between a straight tube (M1) and a conical tube (M5) can be performed by introducing this semi-apical angle into the straight tube. Figure 6 illustrates the force-deformation curve and SEA for the comparison between the straight tube and conical tube. The conical tube results in a lower initial peak load compared to the straight tube, with approximately 25% reduction. The energy absorption capacity of the straight tube is greater than that of the conical tube. However, when the structural mass is considered (indicated by SEA), the SEA results are almost similar for both straight and conical tube because the conical tube is lighter than the straight tube. Therefore, while the conical tube can minimise the initial peak load, it may result in a lower energy absorption capacity compared to the straight tube.

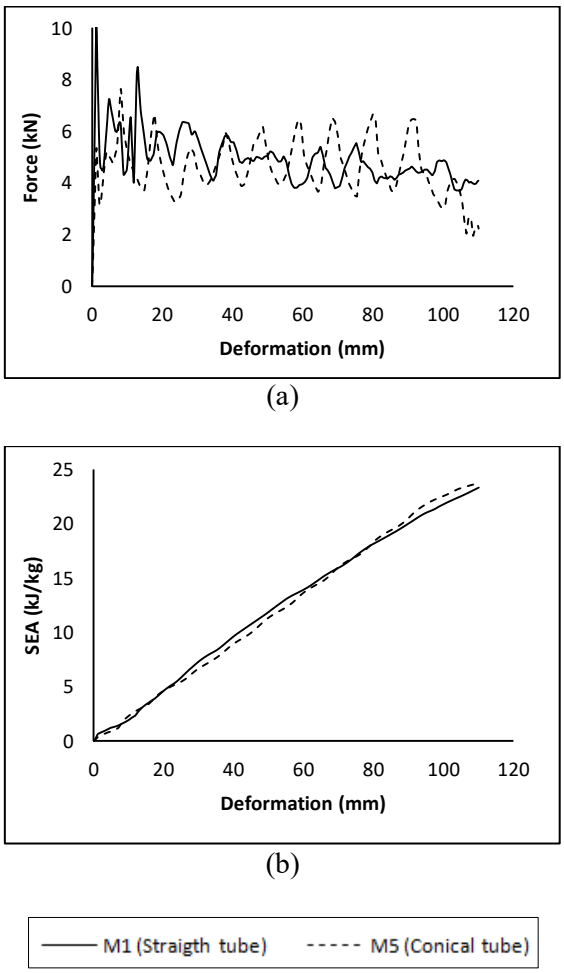

Figure 6. FE model results for the comparison between the straight tube and conical tube: (a) Force-deformation curve and (b) SEA vs. deformation curve.

4.2. Modification of the straight tube

The original straight tube, M1, and the modified straight tubes, M2, M3 and M4, are shown in Figure 7. A horizontal cut with a 10°semi-apical angle from the top is applied in M2. In addition, an end cap was introduced at the top of the straight tube in M3 and M4. A flat end cap was applied in the M3 design, while a hemispherical end cap of 25 mm radius was added in the M4 design.

Figure 7 (a) shows the initial peak loads of the modified tubes are lower than that of the original tube. The initial peak load occurs at a larger deformation length in the M4 design, followed by the M2 and M3 designs, as shown in Figure 7 (a). The occurrence of the initial peak load at a greater deformation length for the modified tubes compared to the original tubes indicates the designs will resist the change in motion, which is significant in reducing the effect of inertia. This result can be achieved by creating a slope or attaching a cap at the top of original tube, as modelled by the design of M2, M3 and M4 tubes.

According to Figure 7 (b), a lower SEA was obtained for the modified tubes compared to the original tube. This result is due to a low mean crushing force obtained during the crushing of the tube. However, the percentage decrease of SEA (14.6%) is less than the percentage decrease in the peak load (28.1%) on average, in the modified tubes compared to the original tube. Thus, the M2, M3 and M4 designs are able to provide better energy absorption characteristics compared to the original tube.

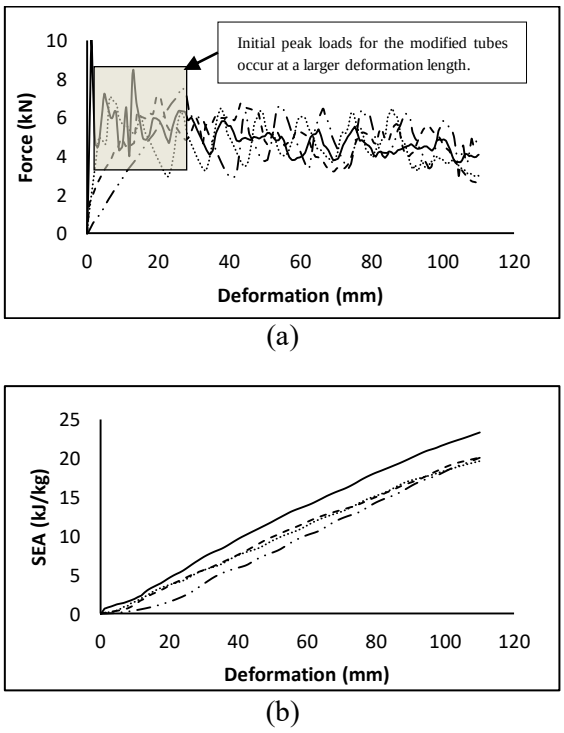

Figure 7. FE model results for the comparison between the original tube (M1) and modified straight tubes (M2, M3 and M4): (a) Force-deformation curve, (b) CFE, and (c) SEA.

4.3. Modification of the conical tube

Three conical tubes, M5, M6 and M7, shown in Figure 5, were created using a 5° semi apical angle. M5 was the original conical tube, a flat end cap and a hemispherical end cap with a 13 mm radius were attached to the top of conical tubes in M6 and M7, respectively. Figure 8 shows a pattern that is similar to that of the straight tube discussed in the previous section. The initial peak loads for the modified conical tubes are lower and the required deformation length to achieve the initial peak load is higher for the modified tube compared to the original tube. Thus, the modified tubes provide more significant results in reducing initial peak load that can provide better crashworthiness structure.

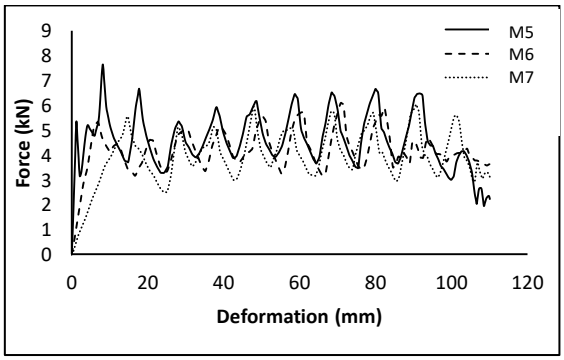

Figure 8. FE model results for the comparison of force-deformation curve between the original conical tube (M5) and the modified conical tubes (M6 and M7).

4.4. Combination of straight, conical and hemispherical tubes in a single tube design

Referring to Figure 5, for the M8 tube, the design includes a conical tube at the top of the straight tube with a 5° semi apical angle and a length of 50 mm. The M9 tube combines the straight and 5° semi apical angle of the conical tube with a hemispherical end cap with a 22 mm radius. The motivation for developing the combination designs in both M8 and M9 is based on previous results that indicated that the straight tube is able to provide optimal energy absorption while the conical tube is better at providing a lower initial peak load. Figure 9 (a) shows the comparison of the force-deformation curves of these modified designs and the original design. The results indicate that these combination designs can lower the initial peak load value by approximately 25% compared to the original straight tube. Moreover, the deformation length required to achieve the first initial peak load in the M9 design increased after introducing the hemispherical cap. In contrast, the energy absorption capacity and SEA for the original straight tube are better than the modified tubes, as shown in Figure 9 (b).

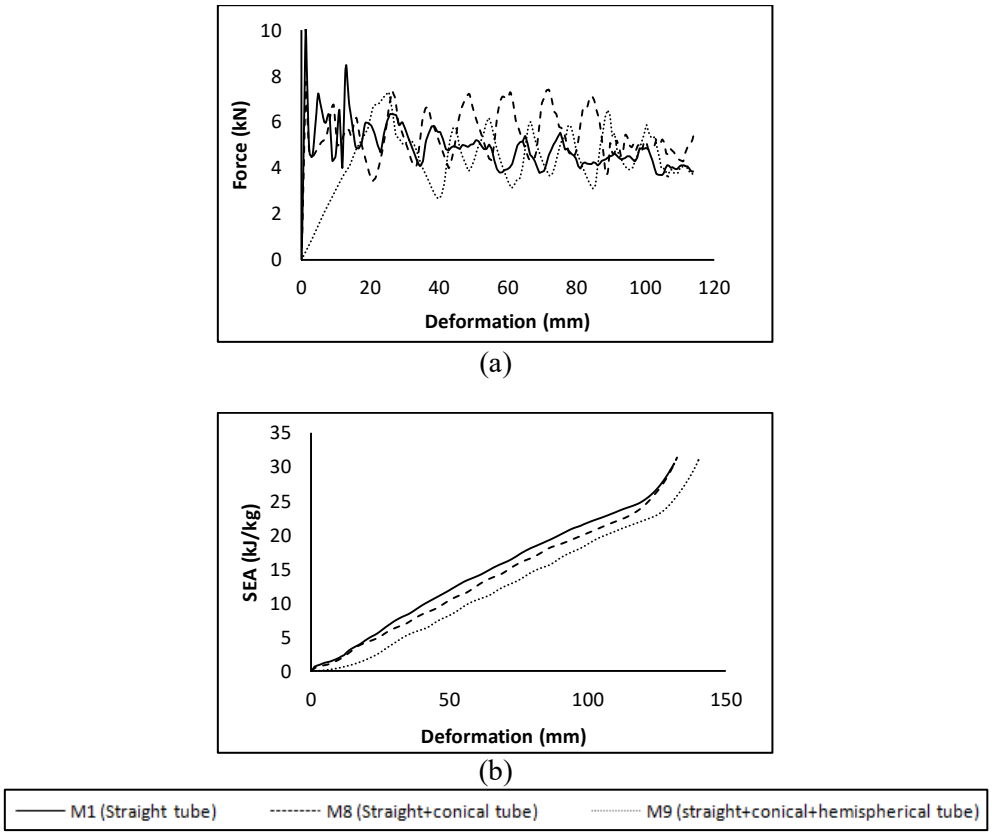

Figure 9. FE model results for the comparison between the original tube (M1) and modified combination tubes (M8 and M9 designs): (a) Force-deformation curve, and (b) SEA vs. deformation.

4.5. Filled straight tube

M10 design represents the straight tube with extruded polystyrene foam that is filled inside the tube. As shown in Figure 10 (a), the energy absorption of the foam-filled tube is greater than that of the empty tube, as seen from the middle until the end stage of the deformation curve. This is due to a low density of foam that influences results in the delay of the foam's effectiveness. The presence of the foam in the tube has an effect at the middle stage of deformation. Thus, the energy absorbed by the foam-filled tube is not enough to offer an optimal SEA value because the mass also increases when the tube is filled with the foam. The inferior SEA values of the foam-filled tube compared to the empty tube are shown in Figure 10 (b).

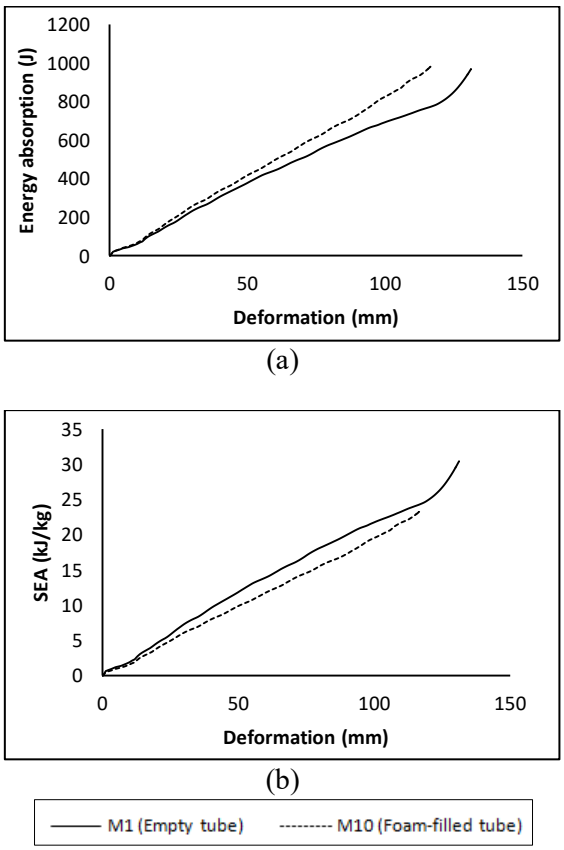

Figure 10. FE model results for the comparison between the empty and foam-filled straight tubes: (a) Force-deformation curve, (b) Energy absorption, and (c) SEA.

4.6. Summary of tube modification

The energy absorption characteristics for all of the tubes were measured until a tube deformation length of 110 mm. Comparisons between the energy absorption characteristics are shown in Figure 11.

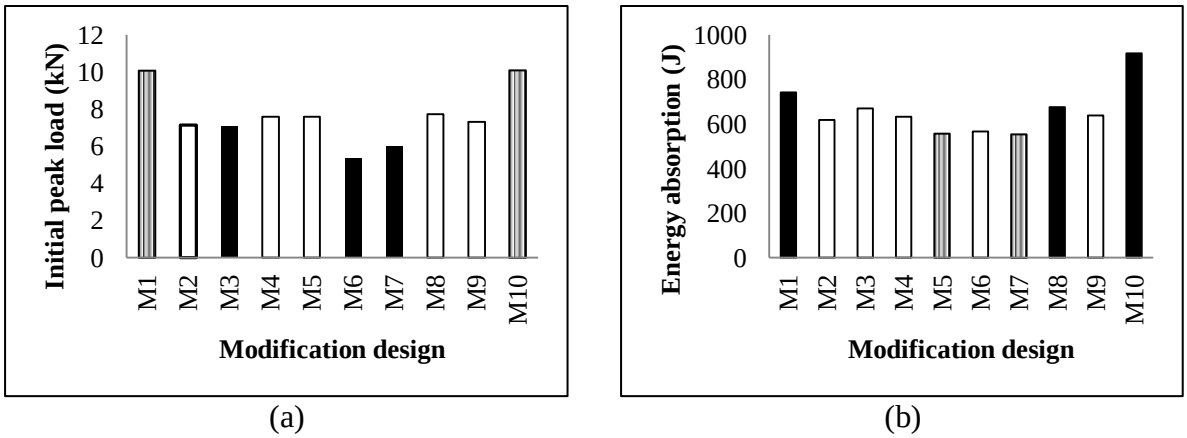

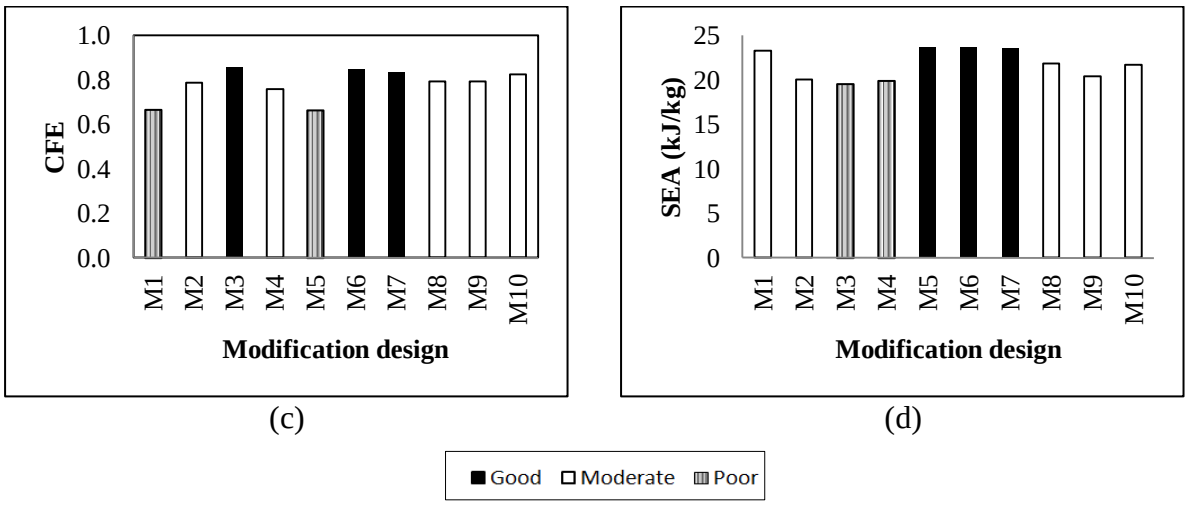

Figure 11. FE model results for the comparison of the energy absorption characteristic among the modification designs: (a) Initial peak load, (b) Energy absorption, (c) CFE and (d) SEA.

As discussed earlier, each modified design has its own advantages and disadvantages in terms of energy absorption characteristics. Overall, the modification designs of M6 (a conical tube with a flat end cap), M8 (a combination of a straight and conical tube) and M9 (a combination of straight and conical tubes with a hemispherical cap) have the best energy absorption characteristics. Specifically, the M6 design, a conical tube with a flat end cap, was identified as the best performing tube among the modified tubes because of its lowest initial peak load, moderate energy absorption capacity and excellent CFE and SEA.

5. Conclusion

In this study, a nonlinear finite element model for the deformation of thin-walled tubes during dynamic axial loading was successfully developed using LS-DYNA. The validity of this nonlinear model was experimentally verified. A good correlation between the finite element model and experimental results was observed. The significant findings obtained from the analysis are summarised below:

a) Modified tubes result in a lower initial peak load for both straight and conical tubes.

b) An empty tube is preferred for the lightweight application as the tube achieves a higher SEA compared to a foam-filled tube. However, when the additional weight is insignificant, such as in a passive protection system, a foam-filled tube is recommended because it can increase the energy absorption capacity.

c) The M6 design, a conical tube with a flat end cap, was identified as the best performing tube among the modified tubes because it had the lowest initial peak load, a moderate energy absorption capacity and an excellent CFE and SEA.

Acknowledgements

The authors are grateful to the Research Management and Innovation Centre and Faculty of Engineering Technology, UniMAP for their financial supports.

References

[1] Shanahan D F 2004 *Basic Principles of Crashworthiness* in *Pathological Aspects and Associated Biodynamics in Aircraft Accident Investigation*, Madrid, Spain.
[2] Alexander J M 1960 An approximate analysis of the collapse of thin cylindrical shells under axial loading *Q J Mech Appl Math,* **13**(1) p10-15.
[3] Sadighi A, Eyvazian A, Asgari M, Magid A H 2019. A novel axially half corrugated thin-walled tube for energy absorption under Axial loading. *Thin-Walled Struct.* **145** p106418.
[4] Kuleyin H, Gumruk R 2019 Pressure wave propagation in pressurized thin-walled circular tubes under axial impact. *Int. J. Impact Eng,* **130** p138-152.
[5] Ferdynus M, Kotelko M, Urbaniak M 2019 Crashworthiness performance of thin-walled prismatic tubes with corner dents under axial impact - Numerical and experimental study. *Thin-Walled Struct,* **144** p106239.
[6] Marzbanrad J, Mehdikhanlo M and Pour A S 2009 An energy absorption comparison of square, circular, and elliptic steel and aluminum tubes under impact loading *Turkish J. Eng. Env. Sci*, **33** p159-166.
[7] Guler M A, Cerit M E, Bayram B, Gerceker B and Karakaya E 2010 The effect of geometrical parameters on the energy absorption characteristics of thin-walled structures under axial impact loading *Int. J. Crashworthiness,* **15**(4) p377-390.
[8] Han H, Taheri F and Pegg N 2007 Quasi-static and dynamic crushing behaviors of aluminum and steel tubes with a cutout *Thin-Walled Struct,* **45**(3) p283-300.
[9] Ghamarian A and Tahaye Abadi M 2011 Axial crushing analysis of end-capped circular tubes *Thin-Walled Struct,* **49**(6) p743-752.
[10] Aktay L, Toksoy A K and Güden M 2006 Quasi-static axial crushing of extruded polystyrene foam-filled thin-walled aluminum tubes: Experimental and numerical analysis *Mater. Des,* **27**(7) p556-565.
[11] Singace A A 2000 Collapse behaviour of plastic tubes filled with wood sawdust *Thin-Walled Struct,* **37**(2) p163-187.
[12] Hallquist J O 2006 *LS-DYNA Theory Manual*. California: Livermore Software Technology Corporation (LSTC).
[13] Ahmad M, Ismail K A and Mat F 2013 Convergence of finite element model for crushing of a conical thin-walled tube *Procedia Eng*, **53**(0) p586-593.
[14] Jones N 1989 *Structural Impact*. Australia: Cambridge University Press.
[15] ASTM 2010 Standard Test Method for Compressive Properties of Rigid Cellular Plastics. United States, *ASTM D1621-10*.